J. ISSAAS Vol. 29, No. 1: 58-74 (2023)

HOMOLOGY MODELING, MOLECULAR DOCKING AND MOLECULAR DYNAMICS STUDY OF TWO DIASTEREOMERS BINDING TO FALL ARMYWORM *SPODOPTERA FRUGIFERDA* ARYLALKYLAMINE N-ACYLTRANSFERASE

Edwin Alcantara*
National Institute of Molecular Biology and Biotechnology (BIOTECH),
University of the Philippines Los Baños, College, Laguna 4031, Philippines
*Corresponding author: epalcantara@up.edu.ph

(Received: October 5, 2022; Accepted: March 5, 2023)

ABSTRACT

The discovery of a new mode of action insecticide is needed to augment existing tools for effective management of fall armyworm (FAW) *Spodoptera frugiferda*. This study sought to investigate the binding mechanism of two diastereomers, PubChem CID 162987453 (D1) and CID 162987454 (D2), to FAW arylalkylamine N-acyltransferase (aaNAT). Homology modeling was performed to predict the 3D structure of the FAW aaNAT receptor. A homology model with the ligands D1 and D2 was used for molecular docking. The docking results were confirmed by molecular dynamics simulation and molecular mechanics Poisson-Boltzmann Surface Area analysis. Finally, per-residue energy decomposition analysis was performed to identify specific amino acid residues involved in ligand binding. Molecular docking revealed the hydrophobic and allosteric binding sites of the two ligands. The binding was stable at 300 ns as shown by molecular dynamics simulation. The binding free energies (ΔG_{bind}) of D1 and D2 were -7.16 kcal/mol and -7.06 kcal/mol, respectively. The hydrophobic residues Ile108 and Leu112 contributed significantly to the binding interaction with D1 and D2, as revealed by per-residue energy decomposition analysis. Together, D1 and D2 are good prime candidates for development as FAW aaNAT allosteric inhibitors.

Key words: sequence alignment, allosteric binding site, inhibitor, hydrophobic, molecular recognition

INTRODUCTION

The fall armyworm (FAW), *Spodoptera frugiferda* is a major insect pest of corn in the Americas and has recently spread to Africa and Southeast Asia (Navasero et al. 2019). FAW is a polyphagous pest that attacks other economically important crops such as sorghum, rice, cotton and vegetables (Hruska 2019). The insect has acquired resistance to many synthetic insecticides (Mota-Sanchez and Wise 2019; Ayil-Gutierrez et al. 2018) including resistance to certain genetically modified (GM) corn events (Monnerat et al. 2018; Huang 2020). Diamides and spinetoram are still generally effective, but resistance to these compounds has been observed in some countries (Gutierrez-Moreno et al. 2019; Okuma et al. 2022). If the trend does not change, the number of available modes of action will be very limited in the future. In the absence of an effective control measure, FAW can spread rapidly after being introduced into an agricultural area (FAO 2020; Wang and Wu 2020).

Insect arylalkylamine N-acyltransferase (aaNAT) is a promising target for the development of new insecticides. Insect aaNAT is responsible for regulating important physiological functions such as cuticle morphology and neural signaling. Inactivation of aaNAT would impair insect survival not only by disrupting neural signaling but also by severe consequences of impaired cuticle development (O'Flynn et al. 2018). Compared to mammals, insects are particularly susceptible to aaNAT inactivation because they lack the enzyme, monoamine oxidase, which functions to inactivate arylalkylamines in mammals (Ganguly et al. 2002). Recent work that provided information on both the 3D structure and critical amino acid residues in the active site of the red flour beetle *Tribolium castaneum* aaNAT (O'Flynn et al. 2020) is an important contribution that could be applied to designing a new insecticide that targets the FAW aaNAT. At the time of this writing, no previous studies describing FAW aaNAT as an insecticidal target have been reported. To date, the IRAC has 32 mode of action classification of insecticides (Sparks et al. 2020). The classification scheme does not include aaNAT inhibitors.

The use of molecular docking and molecular dynamics simulation has been suggested to accelerate the development of new environment friendly insecticides, (Iyison et al. 2021). In fact, it is increasingly being used to study the insecticidal properties of lead compounds (Iyison et al. 2020; Du et al. 2021; Muhseen et al. 2021; Shahraki et al. 2021; Crisan et al. 2022). This has been made possible by recent advances in insect genomics (Asma and Halfon 2021) and computer technology (Buch et al. 2010; Banegas-Luna et al. 2019). The application of computational methods has also become a promising approach to elucidate insect resistance mechanisms (Banba 2021).

Diastereomers are a pair of compounds with the same chemical properties but have different physical properties (Parente et al. 2018). They are stereoisomers that cannot be superimposed and are not mirror images of one another (Nilos et al. 2009). Typically, these compounds are separated using high-performance liquid chromatography (Di Fabio et al. 2013; Kato et al. 2017; Cha et al. 2021). A recent survey of new agrochemicals used as plant protection agents showed that a significant proportion of such products are mixtures of diastereomers (Jeschke 2018). A diastereomeric natural product has recently been reported as a promising FAW insecticide (Silva et al. 2022).

To explore the potential of FAW aaNAT enzyme as a potential target for the development of new insecticides, the three-dimentional (3D) structure of the enzyme must be known. However, the experimentally determined 3D structure of FAW aaNAT is not available in the Protein Data Bank. In the absence of a 3D structure, enzyme structure prediction by homology modeling is a suitable option to enable *in silico* studies (Schmidt et al. 2014). The use of homology models of target insect enzymes has recently been a well-accepted approach to successful screening campaigns for insecticide discovery (Lin et al. 2020; Samurkas et al. 2020; Rodrigues et al. 2021).

This study used homology modeling, molecular docking and molecular dynamics simulation to elucidate the binding mechanism of potential FAW aaNAT inhibitors, focusing on two diastereomers, PubChem CID 162987453 and PubChem CID 162987454 . These two compounds are closely related to the relatively rare dendrodolides for which no insecticidal activity has been reported so far (Sun et al. 2013; Oppong-Danquah 2020). Thus, studying the molecular structure to further decipher the biological function of these unique compounds provides an opportunity to discover a new mode of action insecticide, which is urgently needed to increase the options available for effective management of FAW populations. In addition, the results of this study provide theoretical insights into the molecular recognition of FAW aaNAT inhibitors.

MATERIALS AND METHODS

Target protein receptor. The amino acid sequence of FAW aaNAT protein, heretofore referred to as receptor was obtained from the NCBI database (NCBI 2020) and uploaded to the ModWeb server (Modbase 2020) for homology 3D structure modeling. The 3D structure of the FAW receptor has not

been determined experimentally. Then, the 3D structure of the ModWeb-generated receptor was uploaded to the PREFMD server (PREFMD 2018) for further structure refinement. PREFMD is a protein structure refinement method based on molecular dynamics (Lim and Feig 2018). The refined receptor model was uploaded to the ProBis web server to predict the ligand and its binding site (Konc and Janezic 2010). The position of the allosteric site was predicted using the AlloSite web server (Song et al. 2017). Ramachandran plot analysis of the model receptor was performed using the Molprobity web server (Chen et al. 2010).

Preparation of ligands. The 3D structures of the two diastereomers (PubChem CID 16297453 and PubChem CID 16297454) were obtained from the PubChem compound database in sdf format (Kim et al. 2019). Heretofore, each compound is referred as D1 and D2, respectively. The 2D structure and other molecular properties of these two compounds are shown in Fig. 1.

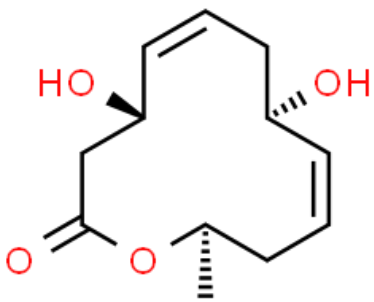

IUPAC Name: (4S,5Z,8R,9Z,12R)-4,8-dihydroxy-12-methyl-1-oxacyclododeca-5,9-dien-2-one
Mol. Wt= 226.27 g/mol
PubChem CID 162987453

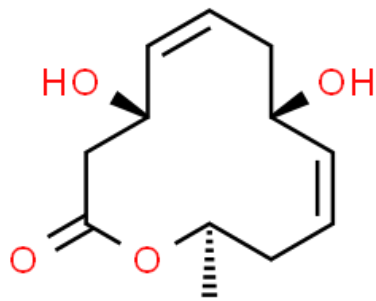

IUPAC Name: (4S,5Z,8S,9Z,12R)-4,8-dihydroxy-12-methyl-1-oxacyclododeca-5,9-dien-2-one
Mol. Wt= 226.27 g/mol
PubChem CID 162987454

Fig. 1. Chemical structure of two diastereomers PubChem CID 16297453 and PubChem CID 16297454 utilized for *in silico* studies. Image source: https://pubchem.ncbi.nlm.nih.gov/compound/

Molecular docking. Molecular docking is a computational tool often used to model the interaction between a small molecule and a protein. The docking process involves predicting the conformation and binding pose as well as the binding affinity of the ligand (Meng et al. 2011). D1 and D2 were docked separately with the model receptor in a previous step using Autodock Vina as implemented in AMDock (Valdes-Tresanco et al. 2020). Each ligand and receptor was protonated at pH 7.3 using the built-in program PDB2PQR. Search space has been set to automatic to enable blind docking. All potential binding sites for each ligand were identified using the built-in AutoLigand program. Blind docking was used to scan the entire receptor surface to identify the predicted allosteric site (Amamuddy et al. 2020). Ligand binding poses in the receptor active site were visualized with LigPlus ver. 2.2.5 (Laskowski and Swindells 2011).

Molecular dynamics (MD). Each bound complex with the highest score from molecular docking study was selected as the starting structure for MD simulation using the software GROMACS version 2020.4 (Abraham et al. 2015). The steps performed for MDS of unbound and bound receptor-ligand complexes, such as topology preparation, system solvation, energy minimization, equilibration and production run, have been previously described (Lemkul 2019). The topology of each ligand was generated using the CGenFF server (Vanommeslaeghe et al. 2010; Yu et al. 2012). The production run for each bound complex was performed for 300 ns on a high performance computing device with 850 CPU cores. A 300 ns MDS iteration was performed for unbound and bound complexes.

Analysis of trajectory files. Trajectory files generated by MD simulations were analyzed using built-in Gromacs utilities. Before the analysis, the periodic boundary condition was removed from the system by using the gmx trjconv tool. The stability of the system was then analyzed with gms rms command. The gyration radius was calculated using gmx gyrate to determine the compactness of the system during the simulation. The number of H-bonds and the distance between receptor and ligand were calculated using gmx hbond. Data were plotted using xmgrace software version 5.1.25 (Cowan and Grosdidier 2000). 500 frames taken from the 1-300 ns MD simulation of each complex were used for both binding free energy and per-residue energy analysis by gmx_MMPBSA (Valdes-Tresanco et al. 2021).

RESULTS AND DISCUSSION

The growing problem of insecticide resistance and the increased risk of beneficial non-target insects being exposed to non-selective synthetic insecticides have prompted crop protection technologists to seek new mode of action insecticides for FAW control. An insecticide that specifically inhibits FAW aaNAT has not yet been developed (Tsugehara et al. 2013). Thus, the identification and development of compounds as FAW aaNAT inhibitors would be an important contribution to the effective management of insecticide resistance in FAW control. Therefore, this study used the available computational tools to investigate the nature of the inhibitory activity of the selected compounds at the insect target site in order to assess its potential to be developed as lead compounds for new insecticidal activity against FAW.

Homology modeling. Homology modeling was used to obtain the model receptor needed for molecular docking of the selected compounds. Homology models have been successfully used for docking analysis (Lohning et al. 2017) and have been shown to be effective when experimental protein structures are not available (Cavasotto 2011). A homology model of the receptor together with the predicted location of the allosteric site is shown in Figure 2A. The putative ligand (i.e., acetyl coenzyme A) and its binding site on the receptor are shown in Figure 2B.

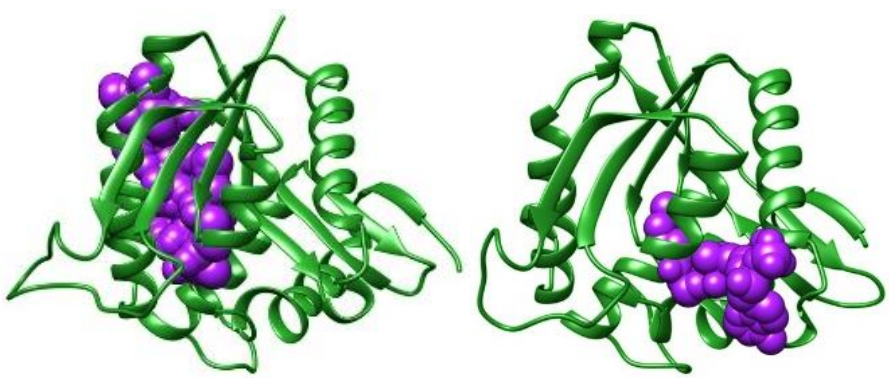

(A) (B)

Fig. 2. (A) Homology model containing the predicted allosteric site (depicted as purple spheres) in fall armyworm *Spodoptera frugiferda* arylalkylamine-N-acyltransferase. The list of allosteric site residues includes the following: Phe30, Glu34, Leu36 Asn37, Leu42, Leu51, Leu52, Gln54, His55, Ser58, Leu84, Asn87, Thr88, Asp89, Ile90, Ser93, Lys96, Glu99, Ile100, Phe105, Ile108, Phe109, Leu112, Tyr113, Asn116, Leu117, Ile119, Asn120, Leu121, Phe122, Lys123, Ile130, Glu132, Ile133, Arg134, Ile135, Lys168, Thr169, Asp170, Thr172. (B) Model protein receptor with bound acetyl coenzyme A (depicted as purple spheres) in the active site. Figures were generated through UCSF Chimera software ver. 1.14 (Pettersen et al. 2004).

Acetyl coenzyme A has previously been shown to play an important role in the catalytic activity of insect aaNATs (Chu-Ya et al. 2020) . The aaNAT 3D structure of the red flour beetle *T. castaneum* (Protein Data Bank I.D. 6V3T) aaNAT was used as a template to build a 3D model of the FAW protein receptor. Based on the results of the ModWeb server (data not shown), the *T. castaneum* template has the highest amino acid sequence identity (34%) with the FAW protein receptor. Amino acid sequence identity below 30% tends to give an inaccurate estimate of the 3D structure of the protein model (Baker and Sali 2001). The Ramachandran plot is used in the final step of structure determination, such as by homology modeling, to identify unrealistic conformations in the model (Hollingsworth and Karplus 2010). The Ramachandran plot represents the distribution of torsion angles phi (Φ) and psi (Ψ) for each amino acid residue in the FAW model receptor (Fig. 3). The distribution of these torsion angles in the diagram indicates that the conformation is energetically favorable (Kleywegt and Jones 1996), because there are no steric clashes between amino acid residues in the predicted model. The plot showed that 98.1%, 100% and 0% of the total residues were in favored regions, in allowed regions and outliers, respectively. The proportion of residues in the favored region (indicated as the inner contour lines in the plot) exceeded the 90% threshold required for a model to be considered highly reliable (Laskowski 1993). The absence of outliers also indicates that no error was introduced into the model during structure refinement.

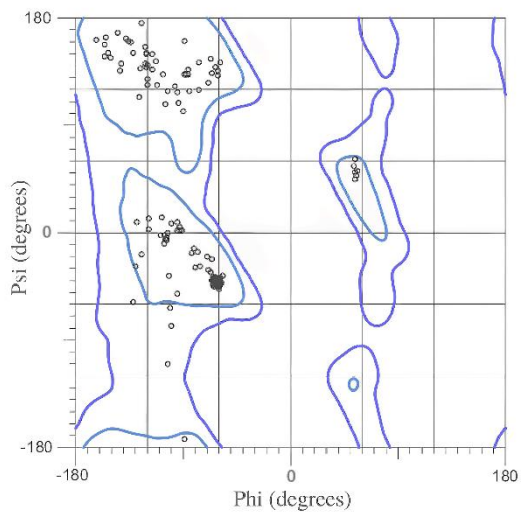

Fig. 3. Ramachandran plot of predicted homology model of fall armyworm *Spodoptera frugiferda* arylalkylamine-N-acyltransferase. Inner blue contour line indicates the favored region, outer purple contour line indicates allowed region. Open circles depict the ϕ,ψ values for each amino acid residue in the model.

Alignment of the sequence with other insect aaNATs (Fig. 4) revealed that the predicted active site of the protein receptor contains eleven highly conserved residues (Phe30, Glu34, Ile135, Leu136, Ser137, Val138, Arg143, Gly144, Gly146, Ala148 and Phe175) which aligned with insect aaNATs such as the red flour beetle, *T. castaneum* (6V3T), the yellow fever mosquito, *Aedes aegypti* (4FD6), and the fruitfly, *Drosophila melanogaster* (3TE4).

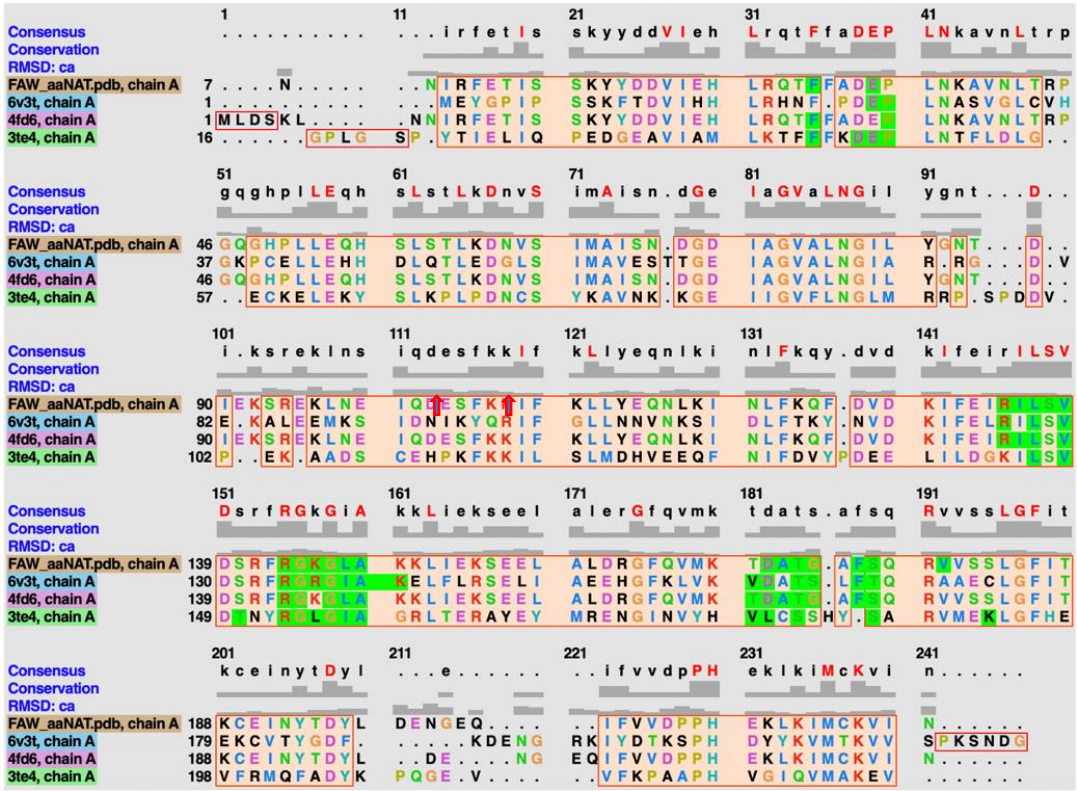

Fig. 4. Sequence alignment of fall armyworm *Spodoptera frugiferda* (FAW_aaNAT.pdb), red flour beetle *Tribolium castaneum* (6V3T), dengue mosquito *Aedes aegypti* (4FD6), and fruitfly *Drosophila melanogaster* (3TE4) arylalkyl N-acyltransferase. Residues highlighted with green background are in interaction with acetyl coenzyme A. Position of predicted hotspot residues Ile108 and Leu112 in protein receptor is indicated by red arrow. Sequence alignment was performed with UCSF Chimera software built-in sequence alignment tool (Petersen et al. 2004).

Corresponding residues of Glu34 in *D. melanogaster* aaNAT (i.e, Glu47), silkworm *Bombyx mori* (i.e., Glu27) and *T. castaneum* (i.e., Glu25) showed critical amino acid residues for catalysis (Cheng et al. 2012; Battistini et al. 2019). Complete loss of enzyme activity resulted from the Phe166Ala mutant in *T. castaneum* aaNAT (O'Flynn et al. 2020). Glu34 and Phe175 are hypothesized to have a similar important function in the active site of the protein receptor. The predicted allosteric site contained the charged amino acids Glu34, His55, Asp89, Lys96, Glu99, Lys123, Glu132, Arg134, Lys168 and Asp170 (Fig. 2A). In addition, seventeen residues were hydrophobic, consisting mainly of leucine and isoleucine.

Molecular docking. The purpose of molecular docking is to predict the conformation of a ligand in its receptor and provide an estimate of the affinity of its interaction (Guedes et al. 2014). In this study, blind docking was performed to identify potential targets of D1 and D2 in the FAW receptor. The estimated LE values indicated that both compounds had a good interaction with the binding site (Table 1).

Table 1. Molecular docking results of *Spodoptera frugiferda* arylalkylamine N-acyltransferase.

Compound code	PubChem ID	Binding affinity (kcal/mol)	K_i (μM)	Ligand efficiency (LE)
D1	CID 162987453	-7.1	6.25	-0.44
D2	CID 162987454	-7.4	3.77	-0.46

The preferential binding of D1and D2 to a common protein receptor target is shown in Figures 5A and 6A. Nine residues (Phe30, Leu36, Leu52, Phe105, Ile108, Leu112, Arg134, Ile135 and Thr172) were in hydrophobic contact with D1. On the other hand, three residues (Glu34, Asn37 and Asp170) were hydrogen bonded with D1. Similarly, nine residues (Leu36, Leu52, His55, Phe105, Phe109, Ile108, Leu112, Ile125, Ile135) were in hydrophobic contact with D2. Three residues (Glu34, Asn37, Arg134) in the binding site were hydrogen bonded with D2. In both cases of binding, the residues are located within the protein receptor (Fig. 5B and 6B).

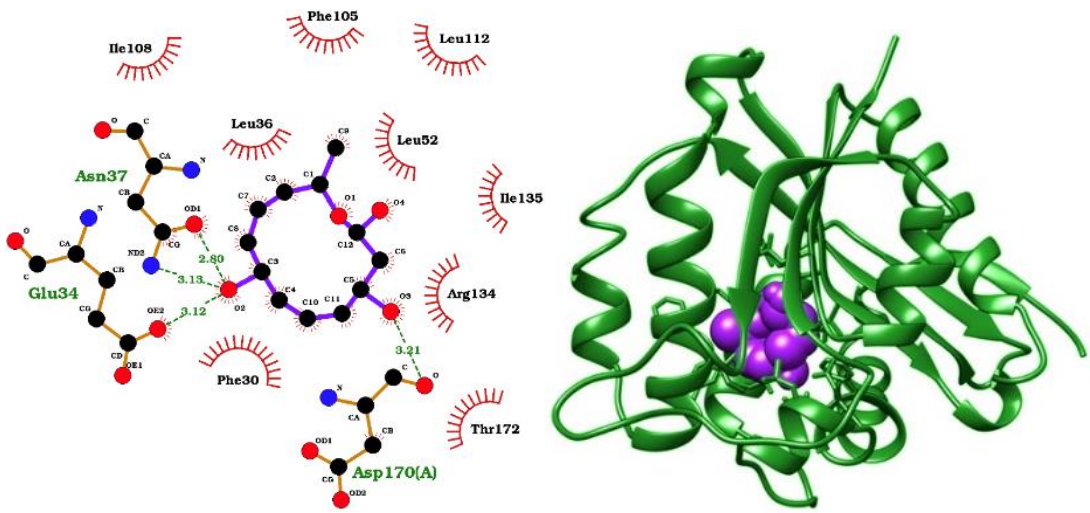

(A) (B)

Fig. 5. Receptor-ligand interaction analysis. A) PubChem compound CID 162987453 (D1)-FAW aaNAT docked complex structure generated through LigPlus ver. 2.2.5 showing hydrogen bonds with Glu34, Asn 37 and Asp170 as green dashed lines and hydrophobic interactions as red arcs. B) PubChem compound CID 162987453 (D1)-FAW aaNAT docked complex structure generated through UCSF Chimera software ver. 1.14 (Pettersen et al. 2004).

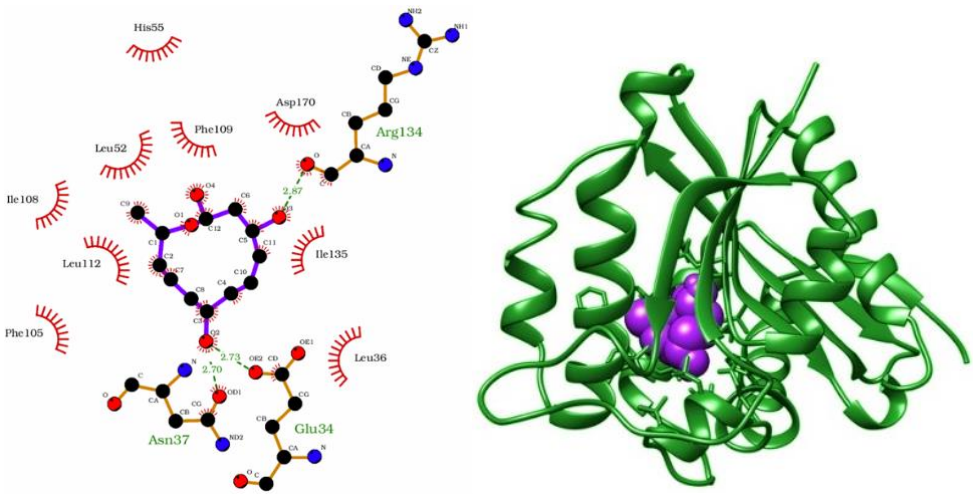

(A) (B)

Fig. 6. Receptor-ligand interaction analysis. A) PubChem compound CID 162987454 (D2)-FAW aaNAT docked complex structure generated through LigPlus ver. 2.2.5 showing hydrogen bonds with Glu34, Asn 37 and Asp170 as green dashed lines and hydrophobic interactions as red arcs. B) PubChem compound CID 162987454 (D2)-FAW aaNAT docked complex structure generated through UCSF Chimera software ver. 1.14 (Pettersen et al. 2004).

Molecular dynamics. All-atom molecular dynamics simulation is a technique that allows understanding the structural dynamics, conformational behavior and stability of proteins and protein-ligand complexes (Hollingsworth and Dror 2018). The root mean square deviation (RMSD) was used to evaluate the overall stability of the system. The RMSD profile of the simulated systems was calculated for protein backbone and is shown in Figure 7A. It can be seen from the plot that the RMSD profile of both the unbound receptor and the bound complexes do not show significant differences. This indicates that the three systems were stable under the given simulation conditions. The RMSD of the unbound receptor (black line) began to increase continuously from 0.1nm beginning at 0 ns to 0.155 nm until 100 ns. Thereafter, the RMSD gradually decreased and stabilized at approximately 0.15 nm from 200 ns to the end of simulation. The RMSD profile of D1-FAW receptor complex (red line) remained stable at approximately 0.15 nm throughout the simulation. The RMSD profile of D2-FAW receptor complex (green line) was similar to that of the unbound receptor. From 0.125 nm at 0 ns, the RMSD increased continuously to 0.2 nm until 100 ns and then, leveled off to 0.15 nm until end of the simulation. No large variations were observed in the simulation, indicating that no significant conformational changes occurred in the three systems (Zrieq et al. 2021). Thus, the convergence shown by the three systems towards an equilibrium state indicated stability. The observed stability may indicate that D1 and D2 are potentially active protein receptor inhibitors. It was previously reported that the molecular stability of the interaction between a compound and its pharmacological target correlates with the actual inhibitory effect (Ramos et al. 2020).

The radius of gyration indicates compactness of a system. The radius of gyration (R_g) of the unbound and bound complexes is shown in Figure 7B. The average R_g value of the two bound complexes was approximately 1.73 nm. The average R_g value of the unbound receptor was approximately 1.71 nm. The slightly higher R_g value of the two bound complexes indicates that the tight binding of D1 and D2 had stabilized the receptor structure. A similar observation has been described previously (Khan et al. 2021).

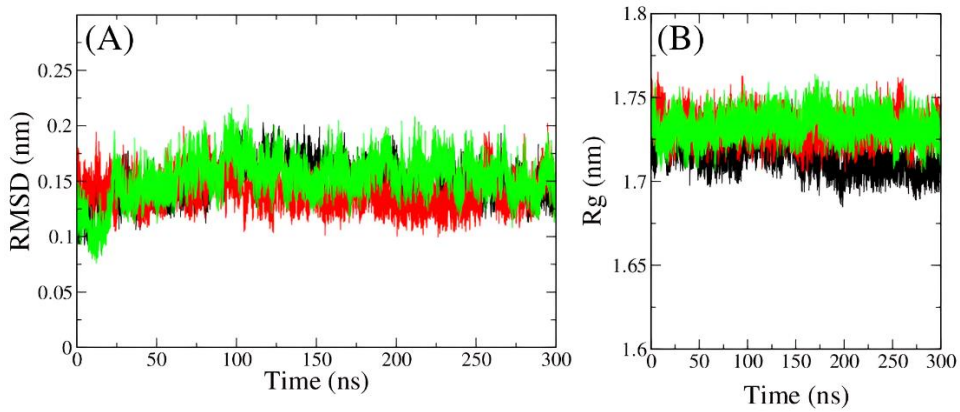

Fig. 7. A) Root mean square deviation of fall armyworm *Spodoptera frugiferda* arylalkyamine-N-acyltransferase during 300 ns MD simulation. Unbound (black), bound ligand D1 (red), bound ligand D2 (green). B) Radius of gyration of fall armyworm *Spodoptera frugiferda* arylalkyamine-N-acyltransferase during 300 ns MD simulation.

Iintermolecular H-bonds were calculated to evaluate the stability of the two bound complexes (Sakthivel et al. 2019). The number of hydrogen bonds present during the simulation between the two bound complexes varied between 1 and 5 H-bonds. The observed hydrogen bonding, which occurred frequently during the simulation, provides further evidence for stable binding of D1 and D2 to the protein receptor (Fig.8A and Fig. 8B).

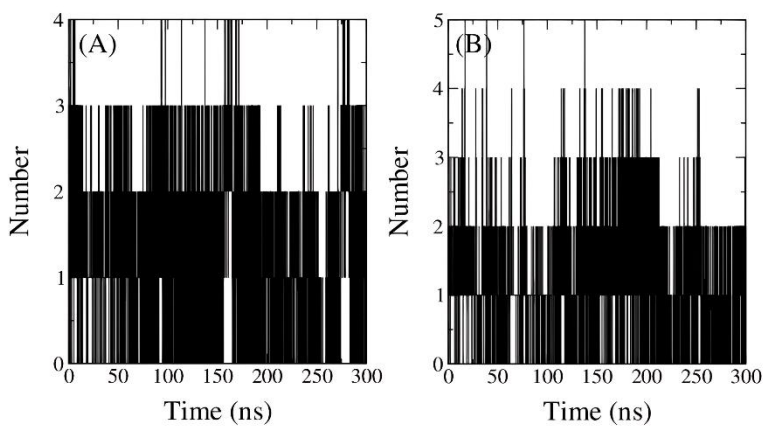

Fig. 8. Number of hydrogen bonds occurring between A) D1 (PubChem CID 162987453) and B) D2 (PubChem CID 162987453) in fall armyworm *Spodoptera frugiferda* arylalkyamine-N-acyltransferase putative allosteric site during 300 ns MD simulation.

Free energy of binding and energy decomposition analysis. The binding affinity of the two diastereomeric compounds obtained from molecular docking was investigated by evaluating the free energy of binding using the MMPBSA method. The total free energy of binding (ΔG_{bind}) components are shown in Table 2. The calculated ΔG_{bind} of both bound complexes indicated favorable binding of D1 and D2 to the protein receptor.

Table 2. Free binding energy of receptor-ligand complexes using MMPBSA method implemented in gmx_MMPBSA, where: energy components contributes to total relative binding energy (ΔG total) of the ligand including van der Waals (VDWAALS) molecular mechanics energy, electrostatic molecular mechanics energy (EEL), polar contribution to the solvation energy (EPB), non-polar contribution of repulsive solute-solvent interactions to the solvation energy (ENPOLAR), non-polar contribution of attractive solute-solvent interactions to the solvation energy (EDISPER), total gas phase (ΔG gas) molecular mechanics energy, total solvation energy (ΔG solv) (Nguyen et al. 2022) .

Complexes	**Free binding energy (kcal/mol) ± standard deviation**							
	VDWAALS	**EEL**	**EPB**	**ENPOLAR**	**EDISPER**	**ΔGGAS**	**ΔGSOLV**	**ΔGTOTAL**
FAW aaNAT-D1	-25.61±2.00	-2.89±1.31	5.35±0.89	-21.44±0.87	37.43±0.92	-28.50±2.00	21.34±1.33	-7.16±2.10
FAW aaNAT-D2	-25.67±2.08	-2.29±1.07	5.14±0.77	-21.69±0.89	37.46±0.90	-27.97±2.13	20.91±1.35	-7.06±2.23

Binding is mainly driven by ΔGGAS in both bound complexes, which consists of van der Waals (VDWAALS) and electrostatic forces (EEL). A large energy contribution from van der Waals forces is expected because the cavity of the protein receptor binding site is mostly lined with hydrophobic residues. Another study found that non-polar interactions exhibit the highest energy in the binding process (Lin et al. 2015). van der Waals forces have been shown to be determinants of the formation and stability of protein-ligand complexes (Humphris and Kortemme 2008; Bitencourt-Ferreira et al. 2019). In both complexes, the effect of electrostatic force on ΔGGAS was small but significant. The estimated total energy of solvation (ΔGSOLV) was not energetically favorable in either complex. ΔGSOLV consists of a polar contribution to the solvation energy (EPB) and a non-polar contribution to the attractive solute-solvent interaction (EDISPER). In addition, the non-polar contribution to the solvation energy (ENPOLAR) from repulsive solute-solvent interactions is favorable for both complexes. Overall, the favorable total gas phase molecular mechanics energy (ΔGGAS) counterbalanced the negative effect of ΔGSOLV, which ultimately affected the favorable ΔG_{bind} of D1 (-7.16±2.10 kcal/mol) and D2 (-7.06±2.23 kcal/mol) binding to the protein receptor. The 0.1 kcal/mol difference in ΔG_{bind} between D1 and D2 seemed negligible. A similar observation was reported previously, where two enantiomers bound to the same allosteric site had only a small difference in binding affinity (Hernandez et al. 2019).

To further elucidate the role of specific residues in ligand binding, a per-residue binding free energy decomposition analysis was performed using the program gmx_MMPBSA. Details of per residue contribution to the binding free energy of the bound complex are shown in Table 3. Most of the interacting residues of both ligands were similar and hydrophobic, consistent with the buried location of the binding site. In particular, the hotspot hydrophobic residues Ile108 and Leu112 made the most important contribution to binding of these two ligands. Ile108 contributed -1.0 kcal/mol and -1.21 kcal/mol to D1 and D2 binding, respectively. Leu112 contributed -1.10 kcal/mol and -1.19 kcal/mol to D1 and D2 binding, respectively. The hotspot residue contributes at least -1.0 kcal/mol to the binding energy of the interaction with the receptor (Humphris and Kortemme 2008). Ile108 is located at conserved sites in four insect aaNATs (Fig. 3). Therefore, it is probably related to the important regulatory function of the protein receptor. Leu112 is a non-conserved residue that may be crucial for binding site selectivity. In addition to stability provided by strong hydrophobic interactions in the binding cavity, the orientation of D1 and D2 to their bound form may result from hydrogen bonds with Asn37 and Arg134, respectively. The electrostatic interaction generated by the hydrogen bond is important because it directs the ligand to its binding form and ensures specific interactions with the complex (Talibov et al. 2021). Thus, both MD simulation and per-residue energy decomposition analysis results confirmed and clarified the docking results.

Table 3. Per-residue energy contributions to the formation of ligand-fall armyworm *Spodoptera Frugiferda* arylalkylamine N-acyltransferase complex.

Complex	**Residues (Per-Residue Energy (kcal/mol±standard deviation)**
D1-FAW aaNAT	Phe30 (-0.58±0.25), Asn37 (-0.58±0.25), Leu52 (-0.67±0.25), His55 (-0.70±0.67), **Ile108** (-1.0±0.24), Phe109 (-0.57±0.22), **Leu112** (-1.10±0.27), Arg134 (-0.81±0.48), Ile135 (-0.87±0.31)
D2-FAW aaNAT	Phe30 (-0.54±0.25), Leu36 (-0.55±0.28), Leu52 (-0.55±0.30), Phe105 (-0.61±0.27), **Ile108** (-1.21±0.30), Phe109 (-0.56±0.23), **Leu112** (-1.19±0.28), Arg134 (-0.82±0.53), Ile135 (-0.82±0.30), Asp170 (0.55±047)

Note: Hot spot residues are shown in bold.

Limitations of the model receptor, docking method (Pantsar and Poso 2018), and MD simulations (Hollingsworth and Dror 2018) do not allow firm conclusions about receptor specificity in this study based on reported results alone. However, the aforementioned simulations can be particularly useful for the design of new FAW insecticides that target a binding site different from the native ligand. For example, simulations have been shown to be able to identify allosteric sites in protein structures (Hollingsworth and Dror 2018). This study further hypothesizes that D1 and D2 bind to the allosteric site of the protein receptor, as suggested by the results of MD and per-residue energy decomposition analyses. Gene cloning and site-directed mutagenesis studies should be performed to confirm the role of Ile108 and L112 in FAW aaNAT allosteric inhibition.

CONCLUSION

The FAW aaNAT binding interaction of D1 and D2 diastereomers was successfully investigated using homology modeling, molecular docking and molecular dynamics simulations. Binding calculations and per-residue energy decomposition analysis showed that hotspot and hydrophobic residues Ile108 and Leu112 played an important role in the molecular recognition of D1 and D2 in the binding site. D2 is a better candidate for development as a lead FAW aaNAT allosteric inhibitor, based on its higher ligand efficiency.

ACKNOWLEDGEMENTS

This study did not receive any specific support from any public, commercial, or not-for-profit funding agency. The author would like to thank the Advanced Science and Technology Institute-Department of Science and Technology for granting free access to the High Performance Computing facility and Elaine De Guzman for help with the figures.

REFERENCES CITED

Abraham, M.J., T. Murtola, R. Schulz, S. Páll, J.C. Smith, B. Hess, and E. Lindahl. 2015. GROMACS: High performance molecular simulations through multi-level parallelism from laptops to supercomputers. SoftwareX. 1:19-25.

Amamuddy, O.S., W. Veldman, C. Manyumwa, A. Khairallah, S. Agajanian, O. Oluyemi, G.M. Verkhivker, and O. T. Bishop. 2020. Integrated computational approaches and tools for allosteric drug discovery. Int. J. Mol. Sci. 21: 847.

Asma, H. and M.S. Halfon. 2021. Annotating the Insect Regulatory Genome. Insects. 12 (7): p.591.

Ayil-Gutiérrez, B.A., L.F. Sánchez-Teyer, F. Vazquez-Flota, M. Monforte-González, Y. Tamayo-Ordoñez, M.C. Tamayo-Ordoñez, and G. Rivera. 2018. Biological effects of natural products against *Spodoptera* spp**.** Crop Prot. 114: 195-207.

Baker, D. and A. Sali. 2001. Protein structure prediction and structural genomics. Science 294 (5540):93-6.

Banba, S. 2021. Application of computational methods in the analysis of pesticide target-site and resistance mechanisms. J. Pestic. Sci. 46 (3): 283-289.

Banegas-Luna, A.J., B. Imbernón, A. Llanes Castro, A. Pérez-Garrido, J.P. Cerón-Carrasco, S. Gesing, I. Merelli, D. D'Agostino, and H. Pérez-Sánchez. 2019. Advances in distributed computing with modern drug discovery. Expert Opin. Drug Discov. 14 (1): 9-22.

Battistini, M.R., B.G. O'Flynn, C. Shoji, G. Suarez, L.C. Galloway, and D.J. Merkler. 2019. *Bm*-iAANAT3: Expression and characterization of a novel arylalkylamine *N*-acyltransferase from *Bombyx mori.* Arch. Biochem. Biophys. 661: 107–116.

Bitencourt-Ferreira, G., M. Veit-Acosta, and W.F. de Azevedo. 2019. Van der Waals potential in protein complexes, pp 79-91. In Docking Screens for Drug Discovery. Humana, New York.

Buch, I., M.J. Harvey, T. Giorgino, D.P. Anderson, and G. De Fabritiis. 2010. High-throughput all-atom molecular dynamics simulations using distributed computing. J. Chem. Inf. Model. 50 (3): 397-403.

Cavasotto, C.N. 2011. Homology models in docking and high-throughput docking. Curr. Top. Med. Chem. 11: 1528-1534.

Cha, J. M., T. H. Lee, L. Subedi, Y. J. Ha, H. R. Kim, S. Y. Kim, S. Choi, and C. S. Kim. 2021. Isolation and structural characterization of four diastereomeric lignan glycosides from *Abies holophylla* and their neuroprotective activity. Tetrahedron 77: 131735.

Chen, V.B., W.B. Arendall, J.J. Headd, D.A. Keedy, R.M. Immormino, G.J. Kapral, W. Murray, J.S. Richardson, and D.C. Richardson. 2010. MolProbity: all-atom structure validation for macromolecular crystallography. Act. Crystallog. Sec. D: Biol. Crystallog. 66:12-21.

Cheng, K.C., J.N. Laio, and P.C. Lyu. 2012. Crystal structure of the dopamine N-acetyltransferase–acetyl-CoA complex provides insights into the catalytic mechanism. Biochem. J. 446: 395–404.

Chu-Ya, W., H. I-Chen, Y. Yi-Chen, D., D. Wei-Cheng, L. Chih-Hsuan, L. Yi-Zong, L. Yi-Chung, C. Hui-Chun, and L. Ping-Chiang. 2020. An essential role of acetyl coenzyme A in the catalytic cycle of insect arylalkylamine N- acetyltransferase. Commun. Biol. 3: 441.

Cowan, R. and G. Grosdidier. 2000. Visualization tools for monitoring and evaluation of distributed computing systems. In Proc. of the International Conference on Computing in High Energy and Nuclear Physics. Padova, Italy.

Crisan, L., S. Funar-Timofei, and A. Borota. 2022. Homology modeling and molecular docking approaches for the proposal of novel insecticides against the African malaria mosquito (*Anopheles gambiae*). Molecules. 27 (12): 3846.

Di Fabio, G., V. Romanucci, C. Di Marino, L. De Napoli, and A. Zarrelli. 2013. A rapid and simple chromatographic separation of diastereomers of silibinin and their oxidation to produce 2, 3-dehydrosilybin enantiomers in an optically pure form. Planta Med. 79 (12): 1077-1080.

Du S., X. Hu, M. Li, X. Jiang, X. Xu, J. Cheng, and X. Qian. 2021. Discovery of novel iminosydnone compounds with insecticidal activities based on the binding mode of triflumezopyrim. Bioorg. Med. Chem. Lett. 46: 128120.

FAO [Food and Agriculture Organization of the United Nations]. Statement on fall armyworm in Sri Lanka. Rome, Italy. http.www.fao.org/srilanka/news/detail-events/en/c/1177796/ (accessed 23 October 2020).

Ganguly, S., S.L. Coon, and D.C. Klein. 2002. Control of melatonin synthesis in the mammalian pineal gland: The critical role of serotonin acetylation. Cell Tissue Res. 1:127-137.

Guedes, I.A., C.S. de Magalhães, and L.E. Dardenne. 2014. Receptor-ligand molecular docking. Biophys. Rev. 6: 75-87.

Gutiérrez-Moreno, R., D. Mota-Sanchez, C. A. Blanco, M. E. Whalon, H. Terán-Santofimio, J. C. Rodriguez-Maciel, and C. DiFonzo. 2019. Field-evolved resistance of the fall armyworm (Lepidoptera: Noctuidae) to synthetic insecticides in Puerto Rico and Mexico. J. Econ. Entomol. 112 (2): 792-802.

Hernández Alvarez, L., D.E. Barreto Gomes, J.E. Hernandez Gonzalez, and P.G. Pascutti. 2019. Dissecting a novel allosteric mechanism of cruzain: A computer-aided approach. PloS one. 14: e0211227.

Hollingsworth, S. A., and P. A. Karplus. 2010. A fresh look at the Ramachandran plot and the occurrence of standard structures in proteins. Biomol Concepts 1: 271-283.

Hollingsworth, S.A. and R.O. Dror. 2018. Molecular dynamics simulation for all. Neuron. 99: 1129-1143.

Hruska, A. J. 2019. Fall armyworm (*Spodoptera frugiperda*) management by smallholders. CABI Rev. 2019: 1-11.

http://feig.bch.msu.edu/prefmd (accessed on May 10, 2021)

https://modbase.compbio.ucsf.edu/modweb/ (accessed on August 15, 2020)

https://www.ncbi.nlm.nih.gov (accessed on August 15, 2020)

Huang, F.N. 2020. Resistance of the fall armyworm, *Spodoptera frugiperda*, to transgenic *Bacillus thuringiensis* Cry1F corn in the Americas: Lessons and implications for Bt corn IRM in China**.** Insect Sci. https://doi.org/10.1111/1744-7917.

Humphris, E.L. and T. Kortemme. 2008. Prediction of protein-protein interface sequence diversity using flexible backbone computational protein design. Structure 16: 1777–88.

Iyison N, A. Shahraki, K. Kahveci, M.B. Düzgün, and G. Gün. 2021. Are insect GPCRs ideal next-generation pesticides: Opportunities and challenges. FEBS J. 288(8):2727-45.

Iyison, N.B., M.G. Sinmaz, B.D. Sahbaz, A. Shahraki, B. Aksoydan, and S. Durdagi. 2020. *In silico* characterization of adipokinetic hormone receptor and screening for pesticide candidates against stick insect, *Carausius morosus*. J. Mol. Graph. and Model. 101: 107720.

Jeschke, P. 2018. Current status of chirality in agrochemicals. Pest Manag. Sci. 74 (11): 2389-2404.

Kato, E., R. Iwata, and J. Kawabata. 2017. Synthesis and detailed examination of spectral properties of (S)-and (R)-higenamine 4′-O-β-d-glucoside and HPLC analytical conditions to distinguish the diastereomers. Molecules 22 (9): 1450.

Khan, A.A., N. Baildya, T. Dutta, and N.N. Ghosh. 2021. Inhibitory efficiency of potential drugs against SARS-CoV-2 by blocking human angiotensin converting enzyme-2: Virtual screening and molecular dynamics study. Mic. Patho. 152: 104762.

Kim, S., J. Chen, T. Cheng, A. Gindulyte, J. He, S. He, Q. Li, B.A. Shoemaker, P.A. Thiessen, B. Yu, L. Zaslavsky, J. Zhang, and E.E. Bolton. 2019. PubChem 2019 update: improved access to chemical data. Nucleic Acids Res. 47: 1102-D1109.

Kleywegt, G. J. and T. A. Jones. 1996. Phi/psi-chology: Ramachandran revisited. Structure. 4 (12): 1395-1400.

Konc, J. and D. Janezic. 2010. ProBiS: a web server for detection of structurally similar protein binding sites. Nucleic Acids Res. 38:W436-40.

Laskowski, R. A., M. W. MacArthur, D. S. Moss, and J. M. Thornton. 1993. PROCHECK: a program to check the stereochemical quality of protein structures. J Appl Crystallogr. 26 (2): 283-291.

Laskowski, R.A. and M.B. Swindells. 2011. LigPlot+: multiple ligand–protein interaction diagrams for drug discovery. J Chem Inf Model. 51 (10): 2778-2786.

Lemkul, J. 2019. From proteins to perturbed Hamiltonians: a suite of tutorials for the GROMACS-2018 molecular simulation package [Article v1. 0]. Living J. Comp. Mol. Sci. 1 (1): 5068.

Lim H. and M. Feig. 2018. PREFMD: a web server for protein structure refinement via molecular dynamics simulations. Bioinf. 34: 1063-1065.

Lin, L., L. Wang, L., and E. Alexov. 2015. On the energy components governing molecular recognition in the framework of continuum approaches. Front. Molecular Sci. 2: 1-12.

Lin, L., Z. Hao, P. Cao, and Z. Yuchi. 2020. Homology modeling and docking study of diamondback moth ryanodine receptor reveals the mechanisms for channel activation, insecticide binding and resistance. Pest Manag. Sci. 76 (4): 1291-1303.

Lohning A.E., S.M. Levonis, B. Williams-Noonan, and S.S. Schweiker. 2017. A practical guide to molecular docking and homology modelling for medicinal chemists. Curr. Top. Med. Chem. 18: 2023-2040.

Meng, X.Y., H.X. Zhang, M. Mezei, and M. Cui. 2011. Molecular docking: a powerful approach for structure-based drug discovery. Curr. Comput. Aided Drug Des. 7: 146-57.

Monnerat, R., E. Martins, C. Macedo, and P. Queiroz. 2018. Evidence of field-evolved resistance of *Spodoptera frugiperda* to Bt corn expressing Cry1F in Brazil that is still sensitive to modified Bt toxins. Plos ONE. 4: e0119544.

Mota-Sanchez, D and J. Wise. Arthropod pesticide resistance database. Michigan State University, East Lansing, MI. https://www. pesticideresistance.org/ (accessed on October 22, 2019).

Muhseen, Z.T., S. Ahmad, and G. Li. 2021. Structural basis of UDP-N-acetylglucosamine pyrophosphorylase and identification of promising terpenes to control *Aedes aegypti*. Colloids Surf. B: Biointerfaces. 204: 111820.

Navasero, M.V., M.M. Navasero, G. Burgonio, K.P. Ardez, M.D. Ebuenga, M. Beltran, M.B. Bato, P.G. Gonzales, G.L. Magsino, B.L. Caoili, and A. Barrion-Dupo. 2019. Detection of the fall armyworm, *Spodoptera frugiperda* (JE Smith)(Lepidoptera: Noctuidae) using larval morphological characters, and observations on its current local distribution in the Philippines. Philipp. Entomol. 33 (2): 171-184.

Nguyen, P.T.V., G. L.T. Nguyen, O.T. Dinh, C.Q. Duong, L.H. Nguyen, and T.N. Truong. 2022. In search of suitable protein targets for anti-malarial and anti-dengue drug discovery. J Mol Struc. 1256: 132520

Nilos, M. G., J. Gan, and D. Schlenk. 2009. Effects of chirality on toxicity, pp 1-21. In B. Ballantyne, T. Marrs, and T. Syversen (eds.). General, Applied and Systems Toxicology. John Wiley & Sons, Ltd.

O'Flynn, B.G., A.J. Hawley, and D.J. Merkler. 2018. Insect arylalkylamine *N*-acetyltransferases as potential targets for novel insecticide design. Biochem. Mol. Biol J. 4: 1-4.

O'Flynn, B.G., E.M. Lewandowski, K.C. Prins, G. Suarez, A.N. McCaskey, N.M. Rios-Guzman, R. L. Anderson, B.A. Shepherd, I. Gelis, J. W. Leahy, Y. Chen, and D. J. Merkler. 2020. Characterization of arylalkylamine N-acyltransferase from *Tribolium castaneum*: An investigation into a potential next-generation insecticide target. ACS Chem. Biol. 15: 513−523.

Okuma, D. M., A. Cuenca, R. Nauen, and C. Omoto. 2022. Large-scale monitoring of the frequency of ryanodine receptor target-site mutations conferring diamide resistance in Brazilian field populations of fall armyworm, *Spodoptera frugiperda* (Lepidoptera: Noctuidae). Insects 13 (7): 626.

Oppong-Danquah, E., P. Budnicka, M. Blümel, and D. Tasdemir. 2020. Design of fungal co-cultivation based on comparative metabolomics and bioactivity for discovery of marine fungal agrochemicals. Marine drugs. 18(2):73.

Pantsar, T. and A. Poso. 2018. Binding affinity via docking: Fact and fiction. Molecules 23: 1899.

Parente, C., C. Azevedo-Silva, R. Meira, and O. Malm. 2018. Pyrethroid stereoisomerism: Diastereomeric and enantiomeric selectivity in environmental matrices- A review. Orb. Electr. J. Chem. 10 (4): 337-345.

Pettersen, E.F., T.D. Goddard, C.C. Huang, G.S. Couch, D.M. Greenblatt, E.C. Meng, and T.E. Ferrin. 2004. UCSF Chimera—a visualization system for exploratory research and analysis. J. Comp. Chem. 25: 1605-12.

Ramos, R., W. Macêdo, J. Costa, C. da Silva, J.C. Rosa, J. Neves da Cruz, M.S. de Oliveira, E.H. de Aguiar Andrade, R. e Silva, R. Souto, and C. Santos. 2020. Potential inhibitors of the enzyme acetylcholinesterase and juvenile hormone with insecticidal activity: study of the binding mode via docking and molecular dynamics simulations. J. Biomol. Struct. Dyn. 38: 4687-4709.

Rodrigues, G.C.S., M. dos Santos Maia, A.B.S. Cavalcanti, R.P.C. Barros, L. Scotti, C.L. Cespedes-Acuna, E.N. Muratov, and M.T. Scotti. 2021. Computer-assisted discovery of compounds with insecticidal activity against *Musca domestica* and *Mythimna separata*. Food Chem. Toxicol. 147: 111899.

Sakthivel, S., S.K. Habeeb, and C. Raman. 2019. Screening of broad spectrum natural pesticides against conserved target arginine kinase in cotton pests by molecular modeling. J. Biomol. Struct. Dyn. 37: 1022-42.

Samurkas, A., X. Fan, D. Ma, R. Sundarraj, L. Lin, L. Yao, R. Ma, H. Jiang, P. Cao, Q. Gao, and Z. Yuchi. 2020. Discovery of potential species-specific green insecticides targeting the lepidopteran ryanodine receptor. J. Agric. Food Chem. 68 (15): 4528-4537.

Schmidt, F., H. Matter, G. Hessler, and A. Czich. 2014. Predictive *in silico* off-target profiling in drug discovery. Future Med. Chem. 6 (3): 295-317.

Shahraki, A., A. Isbilir, B. Dogan, M.J. Lohse, S. Durdagi, and N. Birgul-Iyison, N., 2021. Structural and functional characterization of allatostatin receptor type-C of *Thaumetopoea pityocampa*, a potential target for next-generation pest control agents. J. Chem. Inf. Model. 61 (2): 715-728.

Silva, D. F. da, J. Bomfim, R. C. Marchi, J. C. Amaral, L. S. Pinto, R. M. Carlos, A. G. Ferreira, M. Forim, J.B. Fernandes, M.F. da Silva, R. de Oliveira, D. Buss, W. Kirk, and T.J. Bruce. 2022. Valorization of hesperidin from citrus residues: Evaluation of microwave-assisted synthesis of hesperidin-Mg complex and their insecticidal activity. J. Braz. Chem. Soc. 33 (2022): 772-782.

Song, K., X. Liu, W. Huang, S. Lu, S., and Q. Shen. 2017. Improved method for the identification and validation of allosteric sites. J. Chem. Inf. Mod. 57: 2358-2363.

Sparks, T.C., A.J. Crossthwaite, R. Nauen, S. Banba, D. Cordova, F. Earley, U. Ebbinghaus-Kintscher, S. Fujioka, A. Hirao, D. Karmon, and R. Kennedy. 2020. Insecticides, biologics and nematicides: Updates to IRAC's mode of action classification-a tool for resistance management. Pestic. Biochem. Physiol. 167: 104587.

Sun P., D.X. Xu, A. Mandi, T. Kurtan, T.J. Li, B. Schulz, and W. Zhang. 2013. Structure, absolute configuration, and conformational study of 12-membered macrolides from the fungus *Dendrodochium* sp. associated with the sea cucumber *Holothuria nobilis* Selenka. J Org Chem. 78(14):7030-47.

Talibov, V.O., E. Fabini, E.A. FitzGerald, D. Tedesco, D. Cederfeldt, et al. 2021. Discovery of an allosteric ligand binding site in SMYD3 lysine methyltransferase. ChemBioChem. 22: 1597-1608.

Tsugehara, T., T. Imai, and M. Takeda. 2013. Characterization of arylalkylamine N-acetyltransferase from silkmoth (*Antheraea pernyi*) and pesticidal drug design based on the baculovirus-expressed enzyme. Comp. Biochem. Physiol. C Toxicol. Pharmacol. 157: 93-102.

Valdés-Tresanco, M.S., M.E. Valdés-Tresanco, P.A. Valiente, and E. Moreno. 2020. AMDock: a versatile graphical tool for assisting molecular docking with Autodock Vina and Autodock4. Biol. Direct.15: 1-12.

Valdés-Tresanco, M.S., M.E. Valdés-Tresanco, P.A. Valiente, and E. Moreno. 2021. gmx_MMPBSA: A new tool to perform end-state free energy calculations with GROMACS. J. Chem. Theor. Comp.17: 6281-6291.

Vanommeslaeghe, K., E. Hatcher, C. Acharya, S. Kundu, S. Zhong, J. Shim, E. Darian, O. Guvench, P. Lopes, I. Vorobyov, and A.D. Mackerell Jr. 2010. CHARMM general force field: A force field for drug-like molecules compatible with the CHARMM all-atom additive biological force fields. J. Comp. Chem. 31: 671-690.

Wang F. and H.Y. Wu. More sightings of fall armyworm in Taiwan: COA. http:// focustaiwan.tw/news/asoc/201906160008.aspx (accessed on October 31, 2020).

Yu, W., X. He, K. Vanommeslaeghe, and A.D. MacKerell Jr. 2012. Extension of the CHARMM general force field to sulfonyl-containing compounds and its utility in biomolecular simulations. J. Comp. Chem. 33: 2451-2468.

Zrieq, R., I. Ahmad, M. Snoussi, E. Noumi, M. Iriti, F.D. Algahtani, H. Patel, M. Saeed, M. Tasleem, S. Sulaiman, K. Aouadi, and A. Kadri. 2021. Tomatidine and patchouli alcohol as inhibitors of SARS-CoV-2 enzymes (3CLpro, PLpro and NSP15) by molecular docking and molecular dynamics simulations. Int. J. Mol. Sci. 22: 10693.